

# Probabilistic Risk Assessment Strategy for Damage-Tolerant Composite Spacecraft Component Structural Design

Norman F. Knight Jr.\*

*Veridian Systems Division, Chantilly, Virginia 20151*

and

Edward H. Glaessgen† and David W. Sleight‡

*NASA Langley Research Center, Hampton, Virginia 23681-0001*

**Incorporating risk-based design as an integral part of spacecraft development is becoming more and more common. Assessment of uncertainties associated with design parameters and environmental aspects such as loading provides increased understanding of the design and its performance. Results of such studies can contribute to mitigating risk through a system-level assessment. Understanding the risk of an event occurring, the probability of its occurrence, and the consequence(s) of its occurrence can lead to robust, reliable designs. An approach to risk-based structural design incorporating damage-tolerance analysis is described. The application of this approach to a candidate Earth-entry vehicle is also described. The emphasis is on describing an approach for establishing damage-tolerant structural response inputs to a system-level probabilistic risk assessment.**

## Nomenclature

|                          |  |
|--------------------------|--|
| $[A]$                    | = matrix of constants associated with a given response metric; see Eq. (2) |
| $a_0, a, a_f$            | = crack length, mm   |
| $E_{ii}$                 | = elastic modulus in the $i$ th principal material direction, Pa           |
| $e_{fc}$                 | = failure index for fiber compression; see Eq. (3b)                        |
| $e_{ft}$                 | = failure index for fiber tension; see Eq. (3a)                            |
| $e_{mc}$                 | = failure index for matrix compression; see Eq. (3d)                       |
| $e_{mt}$                 | = failure index for matrix tension; see Eq. (3c)                           |
| $G(a)$                   | = strain energy release rate, $N \cdot m/m^2$                              |
| $G_c$                    | = critical strain energy release rate, $N \cdot m/m^2$                     |
| $G_{ij}$                 | = shear modulus in the $ij$ principal material plane, Pa                   |
| $R_I$                    | = response surface for the $I$ th performance metric                       |
| $R_{MLF}$                | = response surface for the maximum-load-factor performance metric          |
| $R_{SF}$                 | = response surface for the shape-factor performance metric                 |
| $R_{TF}$                 | = response surface for the toughness-factor performance metric             |
| $\{R\}$                  | = vector of values for a given performance metric; see Eq. (2)             |
| $S_{xy}, S_{xz}, S_{yz}$ | = in-plane and transverse shear strength allowables, Pa                    |
| $X_T, X_C$               | = tension and compression strength allowables in the 1-direction, Pa       |
| $x_j$                    | = coded variables for the $j$ th design parameter                          |

|   |  |
|---|--|
| $Y_T, Y_C$                                      | = tension and compression strength allowables in the 2-direction, Pa       |
| $Z_T, Z_C$                                      | = tension and compression strength allowables in the 3-direction, Pa       |
| $\alpha_0, \alpha_k, \alpha_{kl}, \alpha_{klm}$ | = coefficients for response surface approximations; see Eq. (1)            |
| $\{\alpha\}$                                    | = vector of unknown coefficients for a given response metric; see Eq. (2)  |
| $\beta$   | = failure index limit for strength-related failure initiation; see Eq. (3) |
| $\nu_{ij}$                                      | = Poisson's ratios   |
| $\sigma_{ij}$                                   | = stress components, Pa  |

## Introduction

ADVANCED aerospace systems are becoming increasingly more complex, and customers are demanding lower cost, higher performance, and higher reliability. Increased demands are placed on the design engineers to collaborate and integrate design needs and objectives early in the design process to minimize risks that may occur later in the design development stage. The design process itself becomes a balancing process between risk and consequences. High-performance systems require better understanding of system sensitivities much earlier in the design process to meet mission goals. This understanding is developed through enhanced concept selections, heritage data (experience), and enhanced analytical tools. As such, the design of advanced aerospace systems demands a full understanding of system functionality, system interdependencies, system risks, and possible failure scenarios.<sup>1</sup> This understanding of the system cannot be attained from a single discipline view, irrespective of the depth of understanding in that discipline. A systems-engineering perspective with in-depth understanding in at least one discipline critical to the design contributes significantly to understanding and mitigating risk.<sup>1</sup>

Probabilistic risk assessment (PRA) involves the combination and integration of systems engineering, discipline specific analyses, statistics, decision theory, and heritage data. PRA represents a systematic approach for identifying factors and events that have potential to affect mission success and system performance.<sup>2,3</sup> System-level information and integration are needed for a complete vehicle PRA that identifies and prioritizes risk associated with some event. The occurrence of an event, for example, off-nominal condition, subcomponent failure, or accumulation of tolerances, and the severity of the consequences associated with this event can be quantified. Guidance is thereby provided for modifying the design to mitigate known risk to meet specified system requirements for reliability and robustness.

Received 20 February 2002; revision received 15 July 2002; accepted for publication 22 July 2002. Copyright © 2002 by the American Institute of Aeronautics and Astronautics, Inc. The U.S. Government has a royalty-free license to exercise all rights under the copyright claimed herein for Governmental purposes. All other rights are reserved by the copyright owner. Copies of this paper may be made for personal or internal use, on condition that the copier pay the \$10.00 per-copy fee to the Copyright Clearance Center, Inc., 222 Rosewood Drive, Danvers, MA 01923; include the code 0022-4650/03 \$10.00 in correspondence with the CCC.

\*Staff Scientist, Aerospace Engineering Department, 14700 Lee Road. Associate Fellow AIAA.

†Aerospace Engineer, Analytical and Computational Methods Branch, Mail Stop 240. Member AIAA.

The objective of this paper is to describe an approach to risk-based structural design that incorporates damage tolerance. The emphasis of this paper is on the quasi-static response of the spacecraft to launch and entry load cases. Other conditions associated with spectral loading, shock loading, and impact, although readily accommodated by the proposed approach, are not included in the present discussion. The proposed approach incorporates progressive failure analyses and fracture mechanics methods to assess damage tolerance for composite spacecraft systems. Complex, detailed nonlinear finite element simulations are used to evaluate structural integrity for various loading conditions. Selected design parameters are identified as key parameters with some known statistical distribution along with response metrics for the spacecraft mission associated with structural performance. The computational cost of deterministic nonlinear finite element simulations is significant and necessitates an alternate approach for the probabilistic calculations such as response surface methodologies. Multiple response surfaces are proposed for the spacecraft system and its mission. These response surfaces are defined based on the results of deterministic analyses. Each of these steps is described and discussed in detail in the following sections.

### Proposed Risk-Based Design Approach

Mission goals define system requirements, many of which may have direct bearing on the structure, whereas many others may not. Those system requirements that do have a direct bearing on the structure need to be cast into quantifiable design performance or response metrics. In addition, selected design parameters or groupings of design parameters and their statistical variations need to be defined. Probabilistic assessment of the design can then be made using deterministic analysis tools to evaluate the effects of combinations of the input design variables on the response. Through detailed study, the overall design space may then be approximated using response surfaces defining system response metrics developed using large-scale finite element structural analysis simulations.

Hence, the approach to risk-based design incorporating damage-tolerance analyses involves four basic steps. First, response metrics on the structural design performance are developed based on system-level requirements for the vehicle in general and those related to specific disciplines in detail. Understanding system-level requirements and mission goals results in formulating master logic diagrams and functional event sequence diagrams that identify failure scenarios and their consequences due to system uncertainties, limited knowledge or heritage data, or other subsystem failure. Metrics may be explicitly defined within the design documents or may need to be implicitly imposed. After metrics are defined, the designer has measures of success to assess the impact of uncertainties on performance. Second, design parameters that strongly influence the structural performance are defined along with their statistical variation. These statistical variations may be obtained from testing or other sources. These two steps are crystallized by developing event sequence diagrams for structural performance and thereby establishing an understanding of the interplay between subsystems and the structure. Third, response surfaces approximations are developed based on detailed finite element analysis results for use in probabilistic analysis as a fast computational substitute for large-scale finite element simulations. These finite element simulations for specified combinations of the design variables include a damage tolerance assessment and account for material damage, delamination growth, and local stiffness discontinuities. Finally, probabilistic analyses are performed and quantifiable risk measures for mission success are generated and provided to the systems-level probabilistic risk assessment for integration.

### Risk-Based Design

Risk-based design means that uncertainties associated with the design are assessed and their impact determined. Uncertainties may be related to material mechanical properties, geometric shape, loads, or even outside influences that are consequences of other, seemingly unrelated, system response to off-nominal conditions. Robustness implies that the system design is nearly insensitive to these uncertainties, that is, the vehicle design mitigates their influences. Probabilistic methods are used to quantify the occurrence of such events

given certain statistical distributions of design parameters and their mean values. In addition, event sequence diagrams are needed to identify potential critical conditions and to serve as guides to mitigate risk and increase system reliability.

Deterministic analysis tools are commonly used in these assessments to evaluate the structural performance for a given set of design variables and response metrics used to characterize mission success. Deterministic analyses can be simple analytical models or large-scale finite element models. In the latter case, these analyses can overwhelm typical computational infrastructures unless high-throughput computing models (for example, Refs. 4–7) are utilized.<sup>‡</sup> An alternative approach is to employ response surface approximations (for example, Refs. 8–10) that are defined using a selected subset of the design variables and deterministic nonlinear structural analyses. The response surface approximations are then used in the probabilistic risk assessment. To this end, the risk-based design approach studied here utilizes response surfaces defined using a two-level full-factorial model. A two-level factorial design approach defines a first-order response surface with interaction terms. The two-level factorial design approach uses low and high values of selected design variables to define a response surface. For a two-level full-factorial design, the number of deterministic analyses is related to the number of design variables that will later be considered as random variables in the probabilistic analyses. That is, for number of random variables (NRV),  $2^{NRV}$  deterministic analyses are required.

### Damage-Tolerance Analyses

Damage tolerance may be defined as the structure's ability to contain weakening defects under representative loading and to retain adequate residual strength to meet mission requirements.<sup>11</sup> Damage-tolerance analyses are performed to determine the structure's ability to continue to function, in a structural sense, after damage initiation and possible propagation while in service. Damage-tolerance issues for spacecraft systems are critical due to the spacecraft cost and overall program visibility.

Nonlinear finite element simulations of the launch and reentry loading cases provide critical information about the structural design in establishing the reliability of the spacecraft system to achieve its mission. Nonlinear finite element simulations are used to evaluate at least four issues. First, the nonlinear structural analysis simulations are used to determine the extent of the deformations and their gradients. These deformation patterns can be used to validate the assumptions used in the aerodynamic simulations, for example, maintain aerodynamic shape. Second, the nonlinear simulations are used to determine any occurrence of strength-related material failures (i.e., yielding of metal structures or brittle failures for composite materials) and any propagation of damage related to these strength-related failures. Such a simulation is referred to as a progressive failure analysis (PFA). However, initiation of local material failures, although requiring careful study and understanding of their cause, may not prevent the spacecraft from fulfilling its mission. Third, the nonlinear simulations are used to determine whether initial defects (initial delaminations or disbonds) in a spacecraft structure when subjected to launch loading will propagate. These defects or initial damage could be initial delaminations or initial disbonds not detected by nondestructive evaluation (NDE) techniques employed during inspection. This initial damage could also be damage that develops as a result of the launch loads. Fourth, the nonlinear simulations are used to determine whether delaminations or disbonds present at reentry will develop and propagate. The delaminations considered at this step are an accumulation of those associated, perhaps, with manufacturing or fabrication delaminations that are smaller than NDE inspection limits and those that are predicted to occur as a result of the launch loads. Similarly disbonds are associated with a local bond line failure, for example, bonded joints or bonded flanges. Although these two failure modes are different, analysis models often treat them in the same manner.

Hence, the damage-tolerance methodology to be employed for a damage-tolerant spacecraft structural analysis involves two distinct

<sup>‡</sup>Data available online; see Fields, S., "Hunting for Wasted Computing Power—New Software for Computing Networks Puts Idle PC's to Work," accessed 26 August 2002, <http://www.cs.wisc.edu/condor/doc/WiscIdea.html> [last modified 27 November 1996].

phases. One phase predicts strength-related failure initiation and growth that occur during loading. This phase, PFA, is predicted using a two-dimensional classical lamination theory approach with failure initiation criteria and ply discounting (or similar scheme) as the material degradation model. The other phase predicts damage growth from an assumed disbond, delamination, or combination of both that are embedded in the laminate. In addition, strength-related failures may also occur as a result of these embedded flaws. This phase requires using locally refined regions in the finite element model and a strain-energy-release-rate calculation. Each phase typically employs separate structural analysis models with the latter requiring locally refined models to embed the initial damage and monitor its propagation. However, a single finite element model with all structural details (bolt holes, penetrations, flanges, and joints) included could be used in all phases provided the computational infrastructure can deliver the computing resources for the simulations.

**Treatment of Material Damage and Its Propagation**

Nonlinear finite element simulations including progressive failure can be performed using a variety of structural analysis tools as illustrated, for example, by Sleight<sup>12</sup> and Knight et al.<sup>13</sup> Typically, nonlinear finite element analysis tools are used because geometric nonlinearities (large-deflection, large-rotations) are coupled with material nonlinearities (nonlinear elastic, inelastic, brittle damage) in determining the structural response. PFA involves the prediction of local material failure initiation, material degradation, and damage propagation. Failure initiation criteria such as the maximum strain criteria, the Tsai–Wu failure polynomial,<sup>14</sup> or the Hashin criteria<sup>15</sup> are commonly used for laminated composite structures. Many researchers including Singh et al.,<sup>16</sup> Soden et al.,<sup>17</sup> Sleight,<sup>12</sup> and Knight et al.<sup>13</sup> discuss the use and assessment of these failure criteria for laminated composite structures. Continuum damage models based on internal state variables (e.g., Talreja<sup>18</sup>) may also be used but typically require additional material data. If the

spacecraft is fabricated using a process different from lamination of unidirectional plies with various orientations, for example, textile composites or nonpolymeric composites, then other failure models and material degradation models would be employed. Material degradation models also vary depending on the failure criteria, but generally they are based on ply discounting where lamina material stiffness coefficients are reduced in value from their elastic value. Damage propagation requires following the material failure pattern and reestablishing equilibrium as new failures are detected, local material degradation occurs, and stress redistribution develops.

Failure criteria are evaluated at each material point in the composite structure. A material point is defined as a location within the laminate thickness (possibly several points in each ply) and at a given surface location that is defined by a surface integration point or Gauss point for a specific shell element. For example, a single 4-node shell element with 4 surface-integration Gauss points and a 16-ply laminate with 1 sampling point through each layer would have a total of  $4 \times 16 \times 1 = 64$  material points per element. Once failure has been detected, the elastic mechanical properties are degraded to zero (or nearly zero) and archived for use in subsequent calculations. Each material point has a set of state variables that include the failure mode flags (fiber and matrix), the failure index for each mode, an overall failure flag, and the material degradation factor, nine state variables per material point. A holistic PFA methodology<sup>12</sup> shown in Fig. 1 includes material coupon testing to determine material properties, PFA incorporating phenomenological models to predict failure and material degradation within the finite element analysis, and subsequent testing of representative structural configurations to validate the analysis.

**Treatment of Delaminations and Disbonds**

Fracture mechanics methods (e.g., Broek,<sup>19</sup> Aliabadi and Rooke,<sup>20</sup> and Anderson<sup>21</sup>) are used to evaluate whether initial cracks, delaminations, or disbonds will grow and whether that

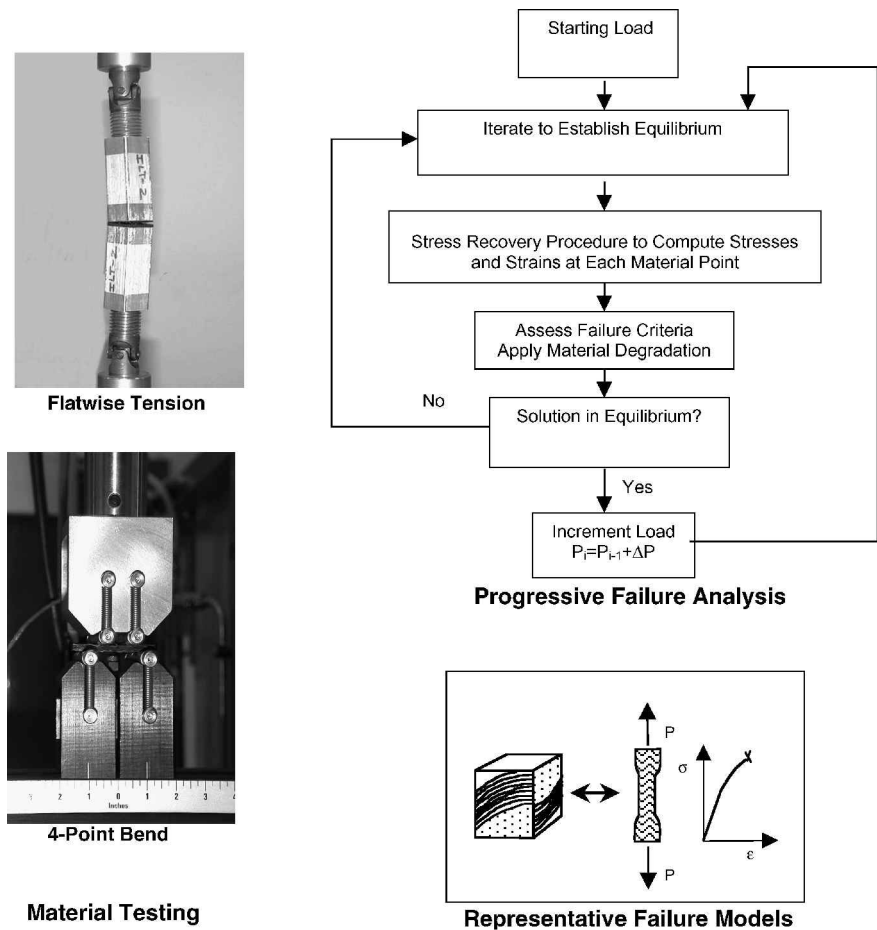


Fig. 1 Components of a holistic progressive failure methodology for composite structures.

growth is stable or unstable. Assessment of disbond or delamination growth is obtained using several computational approaches such as the force method,<sup>22</sup> equivalent domain integral method,<sup>23</sup> virtual crack closure technique (VCCT),<sup>24–26</sup> and the crack tip opening displacement method.<sup>27</sup> The computed strain energy release rates can then be compared to the interlaminar fracture toughness values of the material. The interlaminar fracture toughness is determined for mode I, mode II, and mixed-mode loadings using double-cantilever beam, end notch flexure, and mixed-mode bending configurations, respectively, as indicated in Fig. 2.

Benchmark computational results for two- and three-dimensional analyses, applications to disbond simulations using shear-flexible shell elements, and computational aspects of the method are provided in Refs. 28–36. Once a deterministic finite element analysis has been performed, the fracture mechanics parameters are evaluated. These postprocessing computations of the finite element results are required to calculate the strain energy release rates. As such, an a priori determination of the way the damage will grow is needed, and special attention to local mesh refinement is required. This approach can be coupled with PFA.

Three hypothetical curves of strain energy release rate vs delamination or disbond length ( $G$  vs  $a$ ) are shown in Fig. 3. Hypothetical initial and final delamination or disbond lengths,  $a_0$  and  $a_f$ , respectively, are shown by the vertical solid lines. The initial value  $a_0$  is typically assumed to correspond to the smallest detectable flaw size, whereas the final value  $a_f$  corresponds to a completely delaminated member. Curve A represents a condition where unstable growth may occur because the value of  $G$  is larger than the critical strain-energy-release rate  $G_c$  once the delamination reaches a length  $a'$  corresponding to point  $a_1$  in Fig. 3. In contrast, curve B represents a condition where unstable growth will not occur for any crack length  $a_0 < a < a_f$  because the strain-energy-release rate is

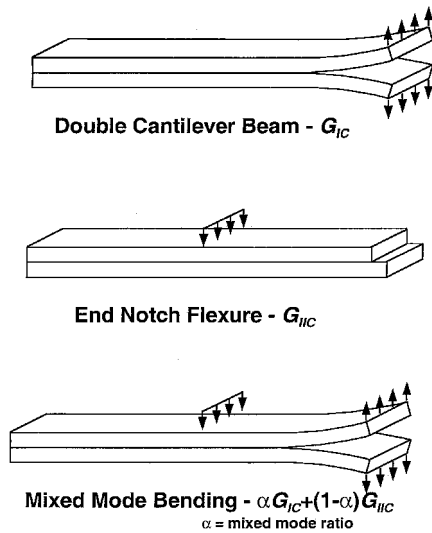


Fig. 2 Fracture mechanics testing for disbonds and delaminations.

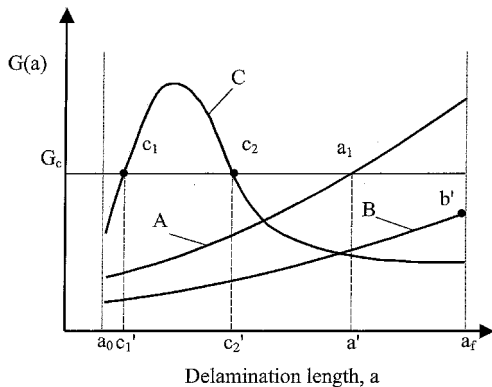


Fig. 3 Strain energy release rate as a function of delamination length.

less than the critical value for the material system for all size delaminations considered. Finally, curve C represents a condition where unstable growth occurs between points  $c_1$  and  $c_2$  ( $c_1' < a < c_2'$ ) and is arrested once the delamination reaches a length  $c_2'$ . Arrest in curve C neglects inertia. (Inertia effects are discussed by Broek.<sup>19</sup>)

Another approach for treating delaminations and disbonds involves the use of recent developments related to decohesion or interface element formulations for strain-softening materials.<sup>37–41</sup> These models require overlaid shell elements in the regions where delaminations and/or disbonds are expected to occur. The decohesion formulation also requires a priori determination of the way the delamination will grow, although the decohesion formulation is not as restrictive as some methodologies. The simulation begins without any delaminations or disbonds. During the simulation, local response may be such that a delamination or disbond initiates and grows. The decohesion element modeling approach provides a computational tool for damage tolerance. This approach can also be coupled with PFA.

### Response Surface Approximations

Each response or performance metric is evaluated for each combination of selected design variables. These results are then used to define a response surface of a given shape.<sup>8–10</sup> Although multiple response functions may be included easily through additional postprocessing of the deterministic analyses, increasing the number of selected design variables has a significant impact on the computational effort. A fundamental assumption in the use of this approach for preliminary design assessment is the functional form of the response surface approximation, that is, first order, second order, or higher order. Implicit assumptions are made regarding the accuracy of the response surface approximation relative to the actual response. The following sections describe a proposed approach to incorporate damage tolerance analysis into the risk assessment by defining appropriate sets of selected design variables and structural performance metrics.

### Design Variable Selection

The selection of design variables to be included in the damage-tolerant risk assessment is a key step in the process. The number and definition of these design variables has two effects. First, selection of variables that influence the structural behavior as reflected in the performance metrics is critical. Second, the number of variables defined relates directly to the magnitude of the computational task, for example, on the order of  $2^{N_{RV}}$  deterministic calculations. For example, the elastic mechanical properties of the composite material ( $E_{11}$ ,  $E_{22}$ ,  $E_{33}$ ,  $G_{12}$ ,  $G_{23}$ ,  $G_{13}$ ,  $\nu_{12}$ ,  $\nu_{23}$ , and  $\nu_{13}$ ) and the strength allowable values ( $X_T$ ,  $X_C$ ,  $Y_T$ ,  $Y_C$ ,  $Z_T$ ,  $Z_C$ ,  $S_{xy}$ ,  $S_{yz}$ , and  $S_{xz}$ ) define 18 independent variables that affect structural performance. In this case each composite material type used in the design would require  $2^{18}$  (or 262,144) deterministic analyses to form a response surface based on a two-level full-factorial approach. For example, if each analysis required 1 min of CPU time, then approximately 182 CPU days would be required. Such an approach does not appear to be tractable at the present time. Therefore, design variables are grouped together, that is, moduli group and strength group, having their own mean values and standard deviations, but sharing a common probability density function. The approach used to incorporate damage tolerance analysis into the risk assessment is to group related design variables together and to assume that all terms in a group share the same statistical distribution, that is, normal distribution or Weibull distribution. Again, if sufficient computing resources are available, each design variable could be treated individually.

### Response Surface Definition

A response surface is a mathematical approximation of a specific system response as a function of a set of design variables.<sup>8–10</sup> A fundamental assumption is required pertaining to the functional form of that surface, that is, first order, second order, or higher order. Multiple response metrics can be involved to assess the robustness and reliability of the system. Development of multiple response surfaces, that is, the number of response surfaces (NRS) to be generated, should require only data extraction or postprocessing of the

deterministic analyses rather than additional simulations. Representation of the  $l$ th response surface (from a total number of NRS) can be expressed as

$$R_l(x_j) = \alpha_0 + \sum_{k=1}^{NRV} \alpha_k x_k + \sum_{k=1}^{NRV} \sum_{l=k+1}^{NRV} \alpha_{kl} x_k x_l + \dots + \sum_{k=1}^{NRV} \sum_{l=k+1}^{NRV} \sum_{m=l+1}^{NRV} \alpha_{klm} x_k x_l x_m + \dots \quad (1)$$

where  $x_j$  represents the coded variable set,  $R_l$  represents the  $l$ th response metric to be “fitted” to a surface (could be up to NRS definitions needed), and  $\alpha_0$ ,  $\alpha_k$ ,  $\alpha_{kl}$ , and  $\alpha_{klm}$  are the unknown coefficients to be determined for the  $l$ th response surface. The coefficients with a single subscript represent first-order terms, and those with two or more subscripts represent the interaction terms for the response surface approximation. The coded variables (normalized physical variables) range in value between  $\pm 1$  and relate to the low and high values of the natural variables (unnormalized physical variables). Response surface approximations of this type involve products of variables but no variable is raised above the first power, that is, no squared terms. This type of response surface is classified as a first-order model with interaction terms.

To determine these coefficients ( $\alpha_0$ ,  $\alpha_k$ ,  $\alpha_{kl}$ , and  $\alpha_{klm}$ ), specific unique combinations of the design variables are defined, and for each combination, the system response is determined: a deterministic analysis typically from which the response metric is extracted, for example, maximum principal strain. The coefficients are then determined by solving a set of linear algebraic equations that is  $2^{NRV} \times 2^{NRV}$  in size and fully populated. When the coded variables are used and  $NRV = 3$  is assumed, eight expressions for a response metric using a two-level, full-factorial approach are needed, and these expressions may be expressed in matrix form as

$$\begin{bmatrix} +1 & -1 & -1 & -1 & +1 & +1 & +1 & -1 \\ +1 & +1 & -1 & -1 & -1 & +1 & -1 & +1 \\ +1 & -1 & +1 & -1 & -1 & -1 & +1 & +1 \\ +1 & -1 & -1 & +1 & +1 & -1 & +1 & +1 \\ +1 & +1 & +1 & -1 & & & & \\ +1 & +1 & -1 & +1 & & \ddots & & \\ +1 & -1 & +1 & +1 & & & \ddots & \\ +1 & +1 & +1 & +1 & +1 & +1 & +1 & +1 \end{bmatrix} \begin{Bmatrix} \alpha_0 \\ \alpha_1 \\ \alpha_2 \\ \alpha_3 \\ \alpha_{12} \\ \alpha_{23} \\ \alpha_{13} \\ \alpha_{123} \end{Bmatrix} = \begin{Bmatrix} R^1 \\ R^2 \\ R^3 \\ \vdots \\ R^8 \end{Bmatrix} \quad (2a)$$

or

$$[A]\{\alpha\} = \{R\} \quad (2b)$$

where  $\{R\}$  is a vector containing the value of the response metric for each combination of the coded variables,  $\{\alpha\}$  is a vector of undetermined coefficients for the response surface, and  $[A]$  is a matrix of constants ( $\pm 1$ s associated with the coded-variable values for each combination). This set of linear algebraic equations can be readily solved using traditional linear equation solvers.

### Application to Earth-Entry Vehicles

To illustrate the outlined approach, application to a candidate Earth-entry vehicle (EEV)<sup>42–44</sup> shown in Fig. 4 is considered. Vehicles of this type are part of the payload for some launch vehicle. Once in orbit, mission objectives are addressed, and the vehicle returns to Earth experiencing loading conditions associated with reentry through the Earth’s atmosphere. Mission success has two aspects. One aspect is the return of science data, and the other aspect is the protection of the biosphere. As a result, reliability and robustness design requirements are extremely high. To mitigate risk and address the impact of possible off-nominal conditions, a scoping PRA was conducted on EEV systems to quantify the risk associated with mission uncertainties.<sup>45</sup> Structural analysis input to the scoping PRA was based on a single performance metric based on the strain at the thermal protection system (TPS)/aeroshell interface bondline using response surface approximations (Kurth, R. E., “Response Surfaces and Statistical Designs for Their Construction,” charts from informal presentation by Battelle to NASA Langley Research Center, EEV Team, Sept. 2000). The present paper addresses one aspect of the design process that contributes to the mission success requirements, namely, structural performance of the EEV aeroshell, a critical driver for EEV structural design.

### Candidate EEV Mission Scenario

Candidate EEV mission scenarios are similar.<sup>42–44</sup> An EEV is launched as a payload on some launch vehicle, it performs its science mission, and then it returns to Earth. The EEV structure has three functions. First, during launch, the EEV structure will react body forces associated with launch accelerations. The EEV will be mounted to the launch vehicle using several hold-down mechanisms (typically bolts) that have the potential to generate severe local stress gradients. Second, during reentry, the EEV structure needs to provide support for the external TPS or may need to serve a multifunctional role for carrying both structural and thermal loads. Third, during reentry, the EEV structure needs to retain its shape for aerodynamic performance and other mission-related aspects.

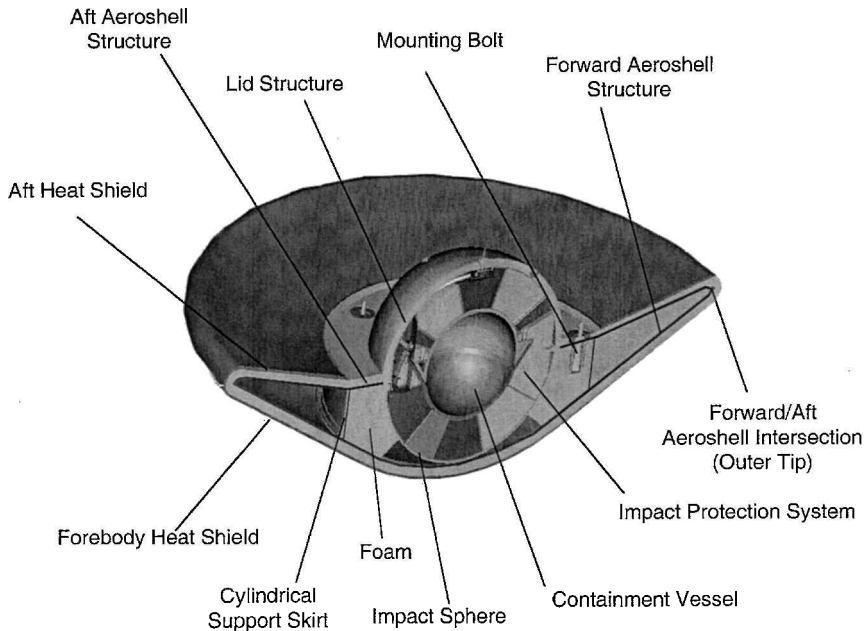


Fig. 4 Candidate EEV system.

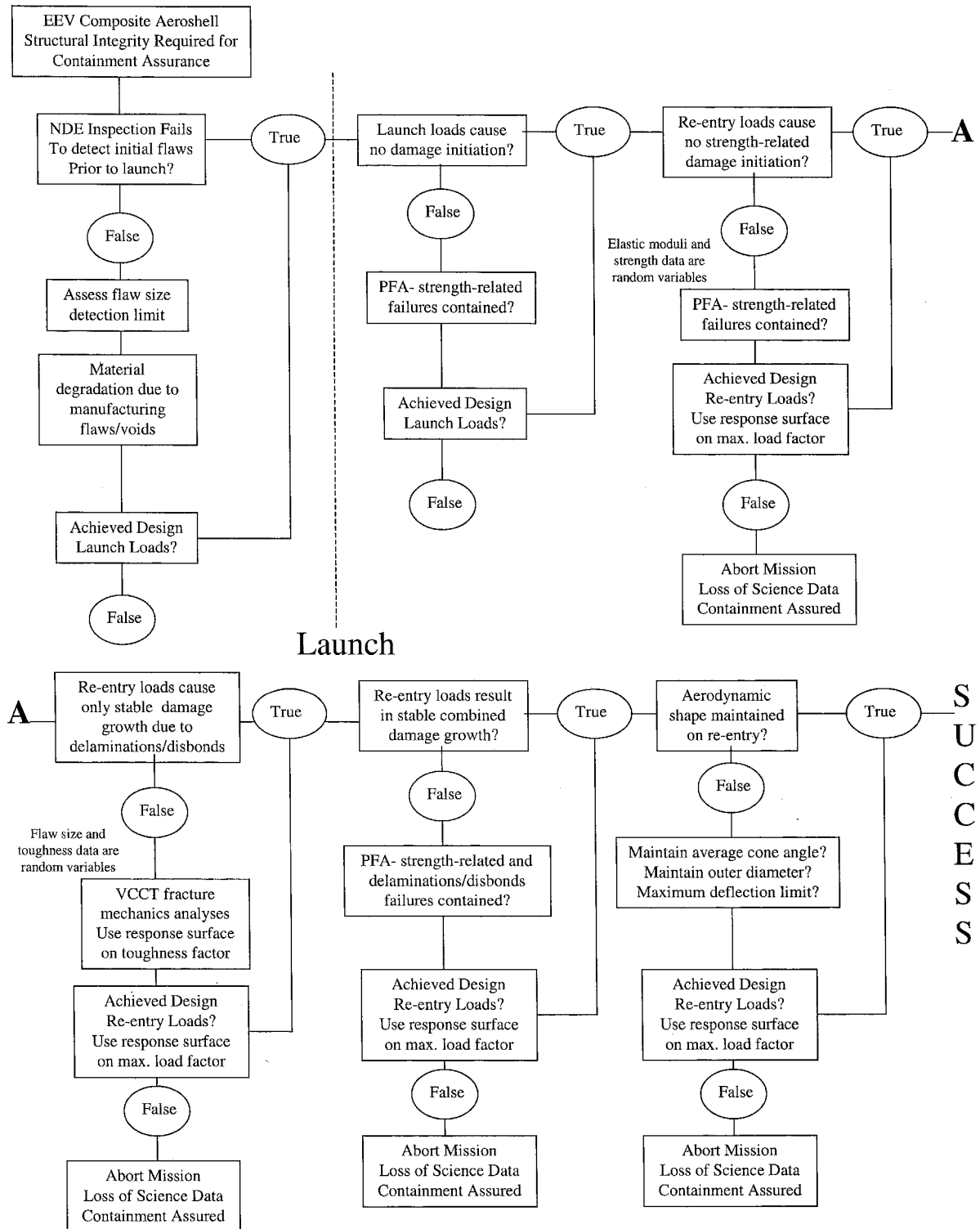


Fig. 5 Representative event sequence diagram for reentry.

To illustrate the approach to risk-based design incorporating damage-tolerance analyses described in the preceding sections, the method is applied to a candidate EEV aeroshell structure. A representative event sequence diagram for this aspect of the design (structural integrity) is presented in Fig. 5. The analyses described provide the necessary input for generating response surfaces that are then used in the probabilistic analyses as indicated on Fig. 5. Impact protection is provided by the impact sphere (e.g., see Kellas<sup>46</sup> for design, fabrication, and testing results and Billings et al.<sup>47</sup> for nonlinear transient dynamic simulations) rather than the aeroshell, and impact protection is not a primary part of the EEV aeroshell structural design problem.

#### Candidate EEV Configuration and Finite Element Modeling

A candidate configuration of an EEV system<sup>44</sup> is a 0.9-m-diam, spherically blunted, 60-deg half-angle cone forebody (Fig. 4). The forebody heat shield is 12 mm thick.

The EEV primary structures include a forward structure, an aft structure, a cylindrical support skirt, a 0.3-m-diam impact shell, and a lid structure (covers the aft side of the impact sphere). These structures are generally thin except near intersections between the internal skirt (support cylinder) and the forward and aft structures, between the forward-aft structures interface (EEV outer tip), and near the three mounting bolts on the aft structure that have metal reinforcement. Dimensions quoted here are representative for the

Table 1 Summary of finite element models used for a typical spacecraft structure

| Finite element model number | Launch load cases     |   |  | Reentry load cases                               |                    |   |
|-----------------------------|-----------------------|---|--|--|--------------------|---|
|                             | Nominal configuration | Nominal material properties and no damage | Nominal material properties and initial damage | Nominal material properties and initiated damage | Initial flaw sizes | Off-nominal flaw sizes and initiated damage |
| 1                           | ✓                     | ✓   |  |  |                    |   |
| 1A                          | ✓                     |   | ✓  |  |                    |   |
| 2                           | ✓                     |   | ✓  | ✓  |                    |   |
| 3A                          | ✓                     |   | ✓  | ✓  | ✓                  |   |
| 3B                          | ✓                     |   | ✓  | ✓  | ✓                  |   |
| 3C                          | ✓                     |   | ✓  | ✓  | ✓                  |   |
| 4                           | ✓                     |   | ✓  | ✓  |                    | ✓   |

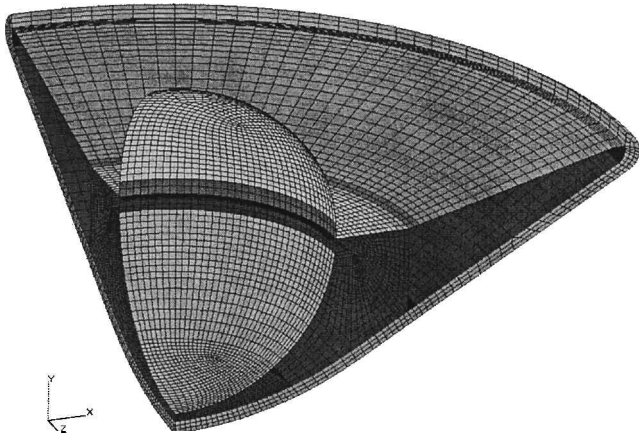


Fig. 6 Representative 90-deg segment of the EEV finite element model.

structures at a conceptual design level. Each component has a near uniform thickness: The forward structure is 2.5 mm thick, the aft structure is 2 mm thick on the sloping section and 4 mm thick in the flat region with the mounting bolt holes, and the skirt is 2 mm thick. Analyses have indicated that for the launch and reentry load cases considered the lid structure and the impact sphere are only lightly loaded and, thus, are considered as linear elastic with no damage in subsequent simulations.

A series of finite element models of a candidate EEV are developed using the geometry definition. A 90-deg segment of one finite element model is shown in Fig. 6 to illustrate the modeling fidelity incorporated into the simulations. The finite element models are assessed to verify modeling assumptions and discretization effects. In this study, the composite structures are modeled using two-dimensional shell elements except near the outer connection between the forward and aft structures (near the EEV outer tip). The foam between the skirt and the impact sphere and the TPS are assumed to have linear elastic behavior and modeled using three-dimensional solid elements. The cylindrical skirt, which bounds the foam and connects the forward and aft aeroshell structures, is modeled using shell elements. Composite structure components are modeled using classical lamination theory, implicit assumption on composite fabrication approach and material constituents, that is, layers of unidirectional polymer-based composite materials.

A certain degree of symmetry does exist in the configuration of the structure and the reentry loading case. However, the launch load cases may cause damage initiation and propagation that are not symmetric. As a result, only full-vehicle finite element models are considered. The reference finite element model, model 1, is defined as a detailed 360-deg model of the EEV having approximately 100,000 elements and 100,000 nodes, over 6,000,000 material points to examine for material damage. In this model, penetrations and the three mounting bolt holes on the aft structure are explicitly modeled and include a local flange for the mounting bolts on the aft structure. Regions of the model for which damage is anticipated, that is, modeled for PFA, have one through-the-thickness integration point per layer.

Increasing this to three points per layer would significantly increase the analysis computing time. Regions of the model for which damage is not anticipated (lid structure and impact sphere) are modeled as elastic only. Various finite element models and their basic use are summarized in Table 1 and discussed further in the “Computational Approach” section.

Before proceeding further, a few comments are in order. First, the commercial structural analysis tools themselves are generally accurate and reliable in terms of correctly performing the calculations. However, few commercial structural analysis tools provide automated adaptive modeling features to ensure accuracy during a nonlinear response simulation, with the possible exception of sheet-metal forming. Second, the material constitutive models including elastic response, failure behavior, and material degradation are limited to common material systems and fabrication types. However, advanced vehicle designs typically use advanced materials technology, for example, three-dimensional woven composites, ceramics, and foams, and direct representation of new materials fabricated using new methods is often only approximate. Finally, prediction of damage-tolerant structural behavior is very complex and problem dependent. Local stress and strain redistributions due to damage initiation and growth will occur and requires automated remeshing techniques or manual remeshing and resolution. Generalizations regarding these aspects of the analysis, especially with regard to correctness and appropriateness, cannot be made.

Loading Cases

There are two loading conditions to be considered in the EEV analysis: launch and reentry. Because a specific launch vehicle is undecided, this uncertainty is addressed by considering eight different launch load cases to envelop the acceleration characteristics of several candidate launch vehicles. Hence, eight different launch load cases are defined and analyzed to account for the uncertainty associated with launch vehicle selection. The reentry loads case is defined based on the likely deceleration of the vehicle on reentry. This load can vary depending on vehicle orientation and trajectory. The reentry loading is considered to be known with certainty.

Selected Design Variables

Design variables having a significant influence on the structural design including damage tolerance are identified and grouped together, if needed. For this study, six groups are identified. The elastic mechanical properties are one group. Another group represents the material strength parameters, whereas another group involves the fracture toughness parameters of the aeroshell material. These three groups are commonly defined as design variables significantly affecting structural performance; however, they do not represent the complete picture. Two additional design variable groups and one load variable group are identified. One design variable group is related to the failure indices for failure initiation (failure index group) and the other is related to initial flaw size for delaminations and disbonds (flaw size group).

The first three groups are defined based on material characterization testing and heritage data for the material system. The fourth group accounts for uncertainty in the failure model. The fifth group

accounts for uncertainty in the initial flaw size in fracture mechanics analyses. The sixth group is based on trajectory and orientation predictions from reentry aerodynamic simulations.

The failure index group involves the failure model and its associated failure modes. For the present approach, HKS/ABAQUS Standard<sup>48</sup> is employed as the nonlinear finite element analysis tool. This tool offers a robust nonlinear solution strategy, ability to incorporate user-defined material models and elements, and a multiprocessor capability. Specific failure models and material degradation models are incorporated through a user-defined constitutive model using UMAT.<sup>48</sup> This material model consists of a two-dimensional classical lamination theory approach with the Hashin failure criteria<sup>15</sup> and ply discounting as the material degradation model. Failure indices for the Hashin criteria are related to fiber and matrix failures and involve four failure modes defined as follows.

Tensile fiber failure:

$$\left(\frac{\sigma_{11}}{X_T}\right)^2 + \left(\frac{\sigma_{12}}{S_{xy}}\right)^2 = e_{ft}^2 \begin{cases} \geq \beta, & \text{failure} \\ < \beta, & \text{no failure} \end{cases} \quad (3a)$$

Compressive fiber failure:

$$\left(\frac{\sigma_{11}}{X_C}\right)^2 = e_{fc}^2 \begin{cases} \geq \beta, & \text{failure} \\ < \beta, & \text{no failure} \end{cases} \quad (3b)$$

Tensile matrix failure:

$$\left(\frac{\sigma_{22}}{Y_T}\right)^2 + \left(\frac{\sigma_{12}}{S_{xy}}\right)^2 = e_{mt}^2 \begin{cases} \geq \beta, & \text{failure} \\ < \beta, & \text{no failure} \end{cases} \quad (3c)$$

Compressive matrix failure:

$$\left[ \left( \frac{Y_C}{2S_{xy}} \right)^2 - 1 \right] \left( \frac{\sigma_{22}}{Y_C} \right)^2 + \left( \frac{\sigma_{22}}{2S_{xy}} \right)^2 + \left( \frac{\sigma_{12}}{S_{xy}} \right)^2 = e_{mc}^2 \begin{cases} \geq \beta, & \text{failure} \\ < \beta, & \text{no failure} \end{cases} \quad (3d)$$

In the Hashin criteria,<sup>15</sup> lamina strength allowables for tension and compression in the lamina principal material directions (fiber or 1-direction and matrix or 2-direction) as well as in-plane shear strength allowable are denoted by  $X_T$ ,  $X_C$ ,  $Y_T$ ,  $Y_C$ , and  $S_{xy}$ , respectively. In-plane normal and shear stress components are denoted by  $\sigma_{ij}$ ,  $i, j = 1, 2$ . Finally, fiber and matrix failure indices for tension and compression ( $e_{ft}$ ,  $e_{fc}$ ,  $e_{mt}$ , and  $e_{mc}$ ) are then compared with a specified limit  $\beta$  to indicate whether failure is predicted. Typically the value of  $\beta$  is unity; however, within the probabilistic risk assessment approach described here,  $\beta$  will be allowed to take on values less than unity in an attempt to account for the uncertainty in the appropriateness of the failure model. One alternative approach to dealing with the uncertainty of the selected failure criteria would be to evaluate concurrently several failure criteria (i.e., maximum strain criteria, Hashin criteria,<sup>15</sup> Tsai–Wu criteria<sup>14</sup>) and then define failure when any criterion is exceeded. Hence, this group varies the failure limit from a value of unity to a smaller value  $\beta$ , that is,  $0 \leq \beta \leq 1$ .

In effect, when  $\beta$  is less than unity, failures would be initiated earlier, that is, at a lower load level, and thereby account, in some sense, for the uncertainty regarding the appropriateness of the selected failure model for the composite material architecture. The approach is to assign this failure limit to all failure modes considered; however, different values could be used for each failure mode or for individual components (fiber or matrix).

The flaw size group involves any and all flaws embedded within the finite element model and associated finite element modeling changes to accommodate these new flaw sizes. Again the flaw size distribution is assumed to be the same for all flaws even though the initial flaw size and its mean value may be different. Based on the VCCT, local computation of strain-energy-release rates uses nodal forces and nodal displacements in the vicinity of the delamination or disbond front. The strain-energy-release rates are computed using locally refined regions in the finite element model at a well-defined interface between layers of the composite material.<sup>28–36</sup>

One final variable is defined as the magnitude of the reentry loading (load variable group). This variable is not directly related to the structure itself but has the potential to affect the results dramatically. The reentry loading condition is a function of other vehicle characteristics on reentry such as spacecraft orientation and reentry trajectory.

The structures' input to the probabilistic risk assessment is based on a series of analyses for both the launch and reentry conditions, as indicated by the event sequence diagrams shown in Fig. 5. Using a two-level full-factorial design model, design parameters are varied from their mean values (a value of +1 for the coded variables) to extreme values, that is, negative two sigma for the physical parameters or a value of −1 for the coded variables. The number of required deterministic analyses increases as  $2^{NRV}$ , where NRV is the number of design variables that will be considered as random during the probabilistic analyses. Results from these analyses are used to define a response surface for each response metric based on two-level full-factorial design approach. The number of required simulations can rapidly become prohibitively high for large-scale finite element models such as the one developed for the candidate EEV (approximately 100,000 nodes). Thus, measures must be taken to ensure all required analyses are performed and to understand how they will be used. Reducing the number of variables will reduce the number of analyses needed, provided the sensitivity of the structural response to the design variables is known and understood.

### Response Metrics

Several response or performance metrics on structural performance may be identified from the event sequence diagrams in Fig. 5 and then analytically defined in relation to mission success. Note that failure initiation, initial flaws, and possible damage propagation do not necessarily result in mission failure. Response metrics are needed that define overall structural failure that would prevent an EEV from accomplishing its mission. The interface between the damage-tolerance analyses and the probabilistic risk assessment is dependent on the variables extracted from the damage-tolerance analyses. Because the number of nodal degrees of freedom and element quantities, that is,  $u_i$ ,  $\varepsilon_{ij}$ ,  $\sigma_{ij}$ ,  $G_I$ ,  $G_{II}$ , etc., is potentially enormous, response metrics for structural response within the probabilistic risk assessment must be computed at the vehicle system level. That is, the damage-tolerant analyses must determine whether or not the vehicle is capable of sustaining launch and reentry loads. Three structural-performance response metrics are considered for an EEV with a composite aeroshell design: a strength-based factor, a toughness-based factor, and a shape-based factor. These factors or response surface parameters for reentry determine whether or not the structural integrity of the EEV has been compromised.

The strength-based factor is taken as the ratio of the largest sustained load at a converged increment in the nonlinear PFA to the reentry design load. This strength-based factor is computed for each combination of design variables and may take on a value equal to or less than unity. A value less than unity, that is, for a load level below the reentry design load, indicates convergence difficulties in the PFA numerical solution due to a discontinuous load path and loss of structural stiffness, and the structure is determined to have failed. Hence, a response parameter  $R_{MLF}$  is defined as a normalized maximum load factor obtained from a PFA simulation for each combination of design variables where a maximum value of unity indicates that, for this combination of design variables, the reentry design load level can be reached. This factor is not directly influenced by the toughness group of design variables. Thus, only four of the design variable groups are used to form the response surface for the maximum load factor. This response surface approximation has the form

$$R_{MLF}(x_1, x_2, x_3, x_4) = \alpha_0 + \sum_{k=1}^{NRV} \alpha_k x_k + \sum_{k=1}^{NRV} \sum_{l=k+1}^{NRV} \alpha_{kl} x_k x_l + \sum_{k=1}^{NRV} \sum_{l=k+1}^{NRV} \sum_{m=l+1}^{NRV} \alpha_{klm} x_k x_l x_m + \alpha_{1234} x_1 x_2 x_3 x_4 \quad (4)$$



This approximation involves 16 unknown coefficients. For the two-level, full-factorial design approach 16 PFA simulations are then required to generate the right-hand-side vector of Eq. (2) and to obtain the coefficients of the response surface defined by Eq. (4).

The toughness-based factor is taken as the ratio of the computed strain energy release rate to the critical value. A response parameter  $R_{TF}$  is defined as a normalized strain energy release rate ( $G/G_c \geq 1$ ) with a value greater than unity indicating unstable damage growth will occur for the specified combination of variables. Values less than unity indicate stable damage growth. This factor is directly dependent on the toughness group; however, the toughness group essentially changes only the critical strain energy release rate, which is compared with a computed strain energy release rate. This increases the number of design variable groups to 5 and increases the number of unknown response surface coefficients to 32. The response surface for the toughness factor is expressed as

$$\begin{aligned}
 R_{MLF}(x_1, x_2, x_3, x_4) = & \alpha_0 + \sum_{k=1}^{NRV} \alpha_k x_k + \sum_{k=1}^{NRV} \sum_{l=k+1}^{NRV} \alpha_{kl} x_k x_l \\
 & + \sum_{k=1}^{NRV} \sum_{l=k+1}^{NRV} \sum_{m=l+1}^{NRV} \alpha_{klm} x_k x_l x_m \\
 & + \sum_{k=1}^{NRV} \sum_{l=k+1}^{NRV} \sum_{m=l+1}^{NRV} \sum_{n=m+1}^{NRV} \alpha_{klmn} x_k x_l x_m x_n + \alpha_{12345} x_1 x_2 x_3 x_4 x_5
 \end{aligned} \quad (5)$$

No additional PFA simulations are required, rather further postprocessing calculations that utilize the 16 PFA simulation results are required to determine the right-hand-side vector of Eq. (2) for the response metric given by Eq. (5).

The shape-based factor determines if the aerodynamic characteristics of the vehicle have been significantly altered due to extensive deformations of the aeroshell even though catastrophic structural damage is not predicted. Calculations use selected points on the EEV model to evaluate average diameter change or change in average angle of the conical shell, or use an  $L_2$  norm of the displacement vector to estimate shape change. A response parameter  $R_{SF}$  is defined as the ratio of some undeformed geometry measure (diameter or cone angle) to the measure computed from the nonlinear simulation. This response surface approximation has the same functional form as that given by Eq. (4). No additional PFA simulations are required; however, a response metric based on geometric shape needs to be evaluated, that is, extract additional information from the previous PFA simulations.

Hence, structural analysis requirements are defined in part from the event sequenced diagrams of Fig. 5 and the definition of the design variables that influence the structural response. In this application, three response metrics are proposed to define structural integrity, namely, the maximum load factor, the toughness factor, and the shape factor. Detailed, finite element analyses are to be performed using deterministic methods and thereby provide the basis for defining associated response surface approximations for each metric. The computational approach to provide this input to the PRA is described next.

#### Computational Approach

The finite element models used for this investigation are described in Table 1. The computational approach begins with the analysis of the eight launch load cases using model 1: a complete vehicle finite element model with nominal material data,  $\beta = 1$ , and without any damage, defects, flaws or imperfections, that is, a model of the pristine structure. Eight PFA simulations are performed where the load factors are gradually increased from zero to a maximum value of unity (representing full application of the design load) for each of the eight launch load cases. A maximum value of unity implies that the structure carried the full magnitude of the load case considered; local damage may be present but did not prevent the PFA simulation of the structural response from converging when the full load was applied. A maximum value less than unity implies that the design loads could not be sustained by the structure. Results include the failure indices from the chosen failure criteria. (Failure modes are grouped as fiber

or matrix failure indices,  $e_f$  and  $e_m$ , respectively.) The fiber failure indices for tension and compression are examined, and the highest value of  $e_{ft}$  and  $e_{fc}$  is then assigned to  $e_f$  (similarly for the matrix failure indices). In addition, the transverse shear strain energy and total strain energy by element are archived. Following each analysis, the failure index distributions by layer in the composite laminate are reviewed, and a cumulative distribution for each failure index, that is, number of elements with a failure index greater than  $\beta$ , is computed. These distributions are used to identify "initiated" imperfection sites. These initiated imperfections simulate possible manufacturing defects or voids with a size defined by the NDE inspection limit (or at least a single element), where the specific failure index causes a corresponding material degradation in those locations. The union of all such initiated imperfection sites are then incorporated into model 1 and called model 1A.

The eight launch load cases are then reanalyzed using model 1A. The results of these PFA simulations are evaluated to see if additional strength-related failures (via the Hashin criteria<sup>15</sup>) have occurred. If no additional strength-related failures are detected beyond those incorporated by changing  $\beta$ , then model 1A defines the baseline finite element model for the reentry load case, that is, model 2. If additional strength-related failures are detected, then the union of all strength-related failures superposed on those already in model 1A becomes the baseline finite element model for reentry, model 2. Hence, the baseline finite element model to study the reentry load case assumes that any manufacturing or fabrication flaws, defects, or delaminations have been detected by NDE inspection. Any initial undetected defect is simulated by material degradation. Furthermore, it is assumed that if the PFA simulations for any launch load case lead to a predicted failure, then design changes would be made before proceeding to analyze the reentry load case. At this point, 16 PFA simulations have been performed.

Next, a PFA simulation is performed using the baseline finite element model, model 2, for the reentry load case. Candidate locations for the initial delaminations are determined by examining the transverse shear strain energy distribution within the model, whereas candidate locations for initial disbands are determined based on assembly and manufacturing information or heritage data. For these identified locations, the baseline finite element model is modified to include locally refined regions to accommodate strain energy release rate calculations using a technique such as the VCCT. Each location may have its own initial size, location, and orientation. Simulation results will need to ensure that these effects do not interact; if they do, then further modifications to the finite element will be required. Incorporating these initial flaws within model 2 leads to model 3A, which reflects these initial flaws plus any and all strength-related failures predicted from the launch load cases.

Three PFA simulations are performed for different flaw sizes (analyze models 3A, 3B, and 3C) to develop a family of curves for strain energy release rate vs flaw size. These results are used to define a nominal value of the flaw size random variable. Model 3A is then modified to reflect the off-nominal flaw sizes and called model 4. This model has nominal material properties for much of the model, nominal geometry, regions with material degradation due to strength-related failures from the launch load cases, and embedded flaws simulating delaminations and disbands.

At this point, 20 PFA simulations have been performed, and the baseline finite element model for reentry (model 3A) has been defined. This finite element model is then used with the reentry load case and each combination of design parameters from the design variable groups to evaluate three response metrics, that is, strength factor, toughness factor, and shape factor. Results obtained using model 3A represent the case of nominal values for each design variable group, including flaw sizes. The off-nominal value for the flaw size and damage from launch require modifications to model 3A that lead to model 4. Off-nominal values of the toughness group require only additional post-processing of the PFA simulation results. Therefore, for the 4 groups of design variables identified (i.e., moduli group, strength group, failure index group, and flaw size group), another 16 ( $2^4$ ) PFA simulations are required for a two-level, full-factorial approach for creating the response surface approximations, giving a total of 36 simulations. Clearly, risk-based design

incorporating damage tolerance requires significant computational effort. Even with the use of response surface approximations, the necessary computations may tax a computing infrastructure. Advanced computing strategies<sup>4-7</sup> need to be harnessed as an enabling infrastructure for the proposed damage-tolerant risk-based design strategy.

To summarize, the computational effort to incorporate damage-tolerant analyses in a probabilistic risk assessment of a candidate EEV structure includes 36 PFA simulations plus selected postprocessing calculations. These simulation results are used to generate the response surfaces corresponding to the three identified response metrics and four groups of random variables for a two-level full-factorial design approach. Additional PFA simulations may be required to investigate some aspect further or to improve the fidelity of the results. Employing the decohesion element modeling approach for delamination and disbond modeling would require 16 additional simulations because the toughness design variable group would be explicitly included as part of the simulations.

### Probabilistic Analyses

The results of these deterministic analyses provide the basis for generating the response surface approximations. A response surface is formed for each structural response metric defined to assess structural performance in meeting mission objectives. The response surfaces are then incorporated into the probabilistic analysis strategy as an approximate method of assessing damage-tolerant structural performance without requiring a full PFA simulation. Each design variable group has an associated statistical distribution function, either known from heritage data, test results, and/or expert opinion. For a specific value of a design variable, the probability of that variable taking on at least that value is known. Collectively the set of design variables is used to determine the corresponding response. Then using their probabilities, the probability of the response reaching at least a certain value can be determined.

### Conclusions

An approach for incorporating damage tolerance analysis with risk-based structural design has been discussed within the context of a candidate EEV composite aeroshell structure. The approach described a process of accounting for local material flaws and strength-related material failures within a probabilistic risk assessment. Progressive failure and fracture mechanics-based analyses are to be performed. Because of the computational effort required to assess the structural integrity of the EEV composite aeroshell structure, design optimization techniques based on response surface approximations are incorporated. In addition, related design variables affecting damage tolerance are grouped together with the same probability distributions.

Nonlinear structural analyses of the EEV structure are to be performed to account for launch and reentry loads in both a pristine state and an imperfect state to establish the damage tolerance of the structure. The design variable groups for the reentry cases include five groups that account for variability in elastic moduli, strength, interlaminar fracture toughness, damage from launch, and delamination/disbond size. Three response metrics are considered including strength, toughness, and vehicle shape to determine the capability of the supporting structure to meet mission goals. When a two-level full-factorial design approach is used, the number of deterministic analyses required to determine the coefficients that define the response surfaces for each response metric is explicitly known. These response surfaces are subsequently used innumerable times in the probabilistic analyses as substitutes for detailed deterministic analyses. The design variable groups will then be treated as random variables in these probabilistic analyses. The approach presented outlines a framework and the steps needed to support a probabilistic risk assessment of damage-tolerant composite structural components of a spacecraft system. However, it should be clearly understood that the simulations and damage models included have implicit assumptions regarding how material failures will initiate and propagate. Accounting for failure mechanisms and damage modes not included in the mathematical models needs to be part of the overall risk assessment.

### Acknowledgment

The work of the first author was supported by the NASA Langley Research Center under Contract GS-35-0038J (Task 1692).

### References

- Blair, J. C., Ryan, R. S., Schutzenhofer, L. A., and Humphries, W. R., "Launch Vehicle Design Process: Characterization, Technical Interaction, and Lessons Learned," NASA TP-2001-210992, May 2001.
- Fragola, J. R., Booth, L., and Shen, Y., "Current Launch Vehicle Practice and Data Base Assessment—Vol. 1: Executive Summary and Report Body," Air Force Systems Command, Rept. AL-TR-89-013, Astronautics Lab., Edwards AFB, CA, June 1989.
- Stamatelatos, M. G., "Overview of Probabilistic Risk Assessment at NASA: Past, Present and Future," *Nondeterministic Approaches and Their Potential for Future Aerospace Systems*, compiled by A. K. Noor, NASA CP-2001-211050, Sept. 2001, pp. 251-276.
- Kaplan, J. A., and Nelson, M. L., "A Comparison of Queueing, Cluster and Distributed Computing Systems," NASA TM-109025, June 1994.
- Basney, J., and Livny, M., "Deploying a High Throughput Computing Cluster," *High Performance Cluster Computing*, edited by R. Buyya, Vol. 1, Prentice-Hall PTR, Upper Saddle River, NJ, 1999, Chap. 5, pp. 116-134.
- Katz, D. S., Cwik, T., Kwan, B. H., Lou, J. Z., Springer, P. L., Sterling, T. L., and Wang, P., "An Assessment of a Beowulf System for a Wide Class of Analysis and Design Software," *Advances in Engineering Software*, Vol. 29, Nos. 3-6, 1998, pp. 451-461.
- Brightwell, R., Fisk, L. A., Greenberg, D. S., Hudson, T., Levenhagen, M., Maccabe, A. B., and Riesen, R., "Massively Parallel Computing Using Commodity Components," *Parallel Computing*, Vol. 26, Nos. 2-3, 2000, pp. 243-266.
- Box, G. E. P., and Draper, N. R., *Empirical Model-Building and Response Surfaces*, Wiley, New York, 1987.
- Cornell, J. A., *How to Apply Response Surface Methodology*, Vol. 8, American Society for Quality Control, Milwaukee, WI, 1990.
- Myers, R. H., and Montgomery, D. C., *Response Surface Methodology: Process and Product Optimization Using Designed Experiments*, Wiley, New York, 1995.
- Sierakowski, R. L., and Newaz, G. M., *Damage Tolerance in Advanced Composites*, Technomic, Lancaster, PA, 1995.
- Sleight, D. W., "Progressive Failure Analysis Methodology for Laminated Composite Structures," NASA TP-1999-209107, March 1999.
- Knight, N. F., Jr., Rankin, C. C., and Brogan, F. A., "STAGS Computational Procedure for Progressive Failure Analysis of Laminated Composite Structures," *International Journal of Non-Linear Mechanics*, Vol. 37, Nos. 4-5, 2002, pp. 833-849.
- Tsai, S. W., and Wu, E. M., "A General Theory of Strength for Anisotropic Materials," *Journal of Composite Materials*, Vol. 5, Jan. 1971, pp. 58-80.
- Hashin, Z., "Failure Criteria for Unidirectional Fiber Composites," *Journal of Applied Mechanics*, Vol. 47, No. 2, 1980, pp. 329-334.
- Singh, S. B., Kumar, A., and Iyengar, N. G. R., "Progressive Failure of Symmetrically Laminated Plates Under Uni-Axial Compression," *Structural Engineering and Mechanics*, Vol. 5, No. 4, 1997, pp. 433-450.
- Soden, P. D., Hinton, M. J., and Kaddour, A. S., "A Comparison of the Predictive Capabilities of Current Failure Theories for Composite Laminates," *Composite Science and Technology*, Vol. 58, No. 7, 1998, pp. 1225-1254.
- Talreja, R., "Modeling of Damage Development in Composites Using Internal Variable Concepts," *Damage Mechanics in Composites*, ASME AD-Vol. 12, American Society of Mechanical Engineers, Fairfield, NJ, 1987, pp. 11-16.
- Broek, D., *Elementary Engineering Fracture Mechanics*, 4th rev. ed., Martinus Nijhoff, Dordrecht, The Netherlands, 1986.
- Aliabadi, M. H., and Rooke, D. P., *Numerical Fracture Mechanics*, Kluwer Academic, Dordrecht, The Netherlands, 1991.
- Anderson, T. L., *Fracture Mechanics: Fundamentals and Applications*, CRC Press, Boca Raton, FL, 1991.
- Raju, I. S., and Newman, J. C., "Three-Dimensional Finite Element Analysis of Finite Thickness Fracture Specimens," NASA TN D-8414, May 1977.
- Nikishkov, G. P., and Atluri, S. N., "Calculation of Fracture Mechanics Parameters for an Arbitrary Three-Dimensional Crack by the 'Equivalent Domain Integral' Method," *International Journal for Numerical Methods in Engineering*, Vol. 24, No. 9, 1987, pp. 1801-1821.
- Rybicki, E. F., and Kanninen, M. F., "A Finite Element Calculation of Stress Intensity Factors by a Modified Crack Closure Integral," *Engineering Fracture Mechanics*, Vol. 9, No. 4, 1977, pp. 931-938.
- Raju, I. S., "Calculation of Strain-Energy Release Rates with Higher Order and Singular Finite Elements," *Engineering Fracture Mechanics*, Vol. 28, No. 3, 1987, pp. 251-274.

<sup>26</sup>Krueger, R., "The Virtual Crack Closure Technique: History, Approach and Applications," NASA CR-2002-211628, April 2002.

<sup>27</sup>Raju, I. S., and Newman, J. C., "SURF3D: A 3D Finite Element Program for the Analysis of Surface and Corner Cracks in Solids Subjected to Mode-I Loadings," NASA TM-107710, 1993.

<sup>28</sup>Wang, J. T., Raju, I. S., Dávila, C. G., and Sleight, D. W., "Computation of Strain Energy Release Rates for Skin-Stiffener Debonds Modeled with Shell Elements," AIAA Paper 93-1501, April 1993.

<sup>29</sup>Wang, J. T., Raju, I. S., and Sleight, D. W., "Composite Skin-Stiffener Debond Analyses Using Fracture Mechanics Approach with Shell Elements," *Composites Engineering*, Vol. 5, No. 3, 1995, pp. 277–296.

<sup>30</sup>Raju, I. S., Sistla, R., and Krishnamurthy, T., "Fracture Mechanics Analyses for Skin-Stiffener Debonding," *Engineering Fracture Mechanics*, Vol. 54, No. 3, 1996, pp. 371–385.

<sup>31</sup>Hitchings, D., Robinson, P., and Javidrad, F., "A Finite Element Model for Delamination Propagation in Composites," *Computers and Structures*, Vol. 60, No. 6, 1996, pp. 1093–1104.

<sup>32</sup>Glaessgen, E. H., Riddell, W. T., and Raju, I. S., "Effect of Shear Deformation and Continuity on Delamination Modeling with Plate Elements," AIAA Paper 98-2023, April 1998.

<sup>33</sup>Glaessgen, E. H., Riddell, W. T., and Raju, I. S., "Nodal Constraint, Shear Deformation and Continuity Effects Related to the Modeling of Debonding in Laminates Using Plate Elements," *Computer Modeling in Engineering and Sciences*, Vol. 3, No. 1, 2002, pp. 103–116.

<sup>34</sup>Chen, D. J., "Efficient Computation of Strain Energy Release Rate in Crack Growth Simulation," *Durability and Damage Tolerance of Composite Structures—1999*, edited by A. A. Pelegri, W. S. Chan, A. Haque, and M. V. Hosur, ASME MD-Vol. 86, AMD-Vol. 232, American Society of Mechanical Engineers, Fairfield, NJ, 1999, pp. 71–78.

<sup>35</sup>Krueger, R., Minguet, P. J., and O'Brien, T. K., "A Method for Calculating Strain Energy Release Rates in Preliminary Design of Composite Skin/Stringer Debonding Under Multi-Axial Loading," NASA TM-1999-209365, July 1999.

<sup>36</sup>Krueger, R., and O'Brien, T. K., "A Shell/3D Modeling Techniques for the Analysis of Delaminated Composite Laminates," *Composites: Part A*, Vol. 32, No. 1, 2001, pp. 25–41.

<sup>37</sup>Chen, J., Crisfield, M., Kinloch, A. J., Busso, E. P., Matthews, F. L.,

and Qui, Y., "Predicting Progressive Delamination of Composite Material Specimens via Interface Elements," *Mechanics of Composite Materials and Structures*, Vol. 6, No. 4, 1999, pp. 301–317.

<sup>38</sup>Gonçalves, J. P. M., de Moura, M. F. S. F., de Castro, P. M. S. T., and Marques, A. T., "Interface Element Including Point-to-Surface Constraints for Three-Dimensional Problems with Damage Propagation," *Engineering Computations*, Vol. 17, No. 1, 2000, pp. 28–47.

<sup>39</sup>Dávila, C. G., Camanho, P. P., and de Moura, M. F., "Mixed-Mode Decohesion Elements for Analysis of Progressive Delaminations," AIAA Paper 2001-1486, April 2001.

<sup>40</sup>Goyal, V. K., Jaunky, N., Johnson, E. R., and Ambur, D., "Intralaminar and Interlaminar Progressive Failure Analyses of Composite Panels with Circular Cutouts," AIAA Paper 2002-1745, April 2002.

<sup>41</sup>Camanho, P. P., Dávila, C. G., and Ambur, D. R., "Numerical Simulation of Delamination Growth in Composite Materials," NASA TP-2001-211041, Aug. 2001.

<sup>42</sup>Mitcheltree, R. A., Kellas, S., Dorsey, J. T., Desai, P. N., and Martin, C. J., "A Passive Earth-Entry Capsule for Mars Sample Return," AIAA Paper 98-2851, June 1998.

<sup>43</sup>Desai, P. N., Mitcheltree, R. A., and Cheatwood, F. M., "Sample Return Missions in the Coming Decade," International Astronautics Federation Congress, Paper IAF-00-Q.2.04, Oct. 2000.

<sup>44</sup>Mitcheltree, R., Braun, R., Hughes, S., and Simonsen, L., "Earth Entry Vehicle for Mars Sample Return," International Astronautics Federation Congress, Paper IAF-00-Q.3.04, Oct. 2000.

<sup>45</sup>Fragola, J., Minarick, J. W., Putney, N., and Yazdipour, S., "Scoping Risk Assessment: Earth Entry Vehicle for the Mars Sample Return Mission," Science Applications International Corp., New York, March 2000.

<sup>46</sup>Kellas, S., "Design, Fabrication and Testing of a Crushable Energy Absorber for Passive Earth Entry Vehicle," NASA CR-2002-211425, 2002.

<sup>47</sup>Billings, M. D., Fasanella, E. L., and Kellas, S., "Impact Test and Simulation of Energy Absorbing Concepts for Earth Entry Vehicles," AIAA Paper 2001-1602, April 2001.

<sup>48</sup>"ABAQUS/Standard User's Manual," Ver. 5.6, Vol. 3, Hibbitt, Karlsson and Sorenson, Pawtucket, RI, 1996.

M. S. Lake  
Associate Editor